Manufacturing Letters 14 (2017) 6–9

Contents lists available at ScienceDirect

Manufacturing Letters

journal homepage: www.elsevier.com/locate/mfglet

Letters

Selective laser melting of fiber-reinforced glass composites

Ninggang Shen, Avik Samanta, Qinghua Wang, Hongtao Ding *

Department of Mechanical and Industrial Engineering, University of Iowa, Iowa City, IA 52242, USA

ARTICLE INFO

Article history:
Received 2 August 2017
Accepted 13 September 2017
Available online 28 September 2017

Keywords:
Fiber-reinforced glass composite
Selective laser melting
Fibers
Glass powder
Microstructure

ABSTRACT

A selective laser melting (SLM) process is developed for manufacturing of a novel glass fiber-reinforced glass (GRFG) composite material. Experiments using a continuous wave fiber laser are conducted for demonstrating this SLM process using borosilicate S-glass fibers and fine soda lime glass powders, which have distinct glass transition temperatures. During laser scanning, fine glass powders turn into viscous flow. The molten glass flows through and encapsulates the relatively solid fibers, which are not fused due to their relatively higher glass transition temperature. Upon cooling, a compacted GRFG composite forms with a high volume ratio of intact and well-encapsulated glass fibers.

1. Introduction

Fiber-reinforced glass (FRG) composite is a new type of composite material for structural and optical applications [1–4]. For instance, Boccaccini and his colleagues developed a transparent glass fiber-reinforced glass (GFRG) composite material using a hot-pressing process [5–8]. From their process, a laminate composite structure is achieved with unidirectional glass fibers sandwiched between glass slides. The resultant laminate structure had a low volume ratio of 5%–10% for fibers, which limits its capability of further improving fracture toughness. In addition, significant debonding and fiber pull-outs were observed in the microstructure. Yao and his colleagues developed a laser-based glass fusion reinforcement process for glass fiber-reinforced polymers [9–12]. In their work, a soda lime glass bead of $\sim$1 mm in diameter was placed on top of multiple glass fabric layers and melted using a Nd:YAG laser. A large glass joint about 1 mm in diameter was formed after solidification, which melted a large area of glass fibers. More recently, fused deposition modeling (FDM)-based additive manufacturing (AM) processes have been developed for manufacturing optical transparent glass using soda lime glass nuggets [13] or solid filament [14].

In this study, a novel selective laser melting (SLM) process is presented for manufacturing of a new glass fiber-reinforced glass (GRFG) composite material. To demonstrate this SLM process, a continuous wave fiber laser is employed to scan a glass powder bed, in which glass fibers are embedded. Borosilicate S-glass fibers and fine soda lime glass powders with distinct glass transition temperatures are investigated as fiber reinforcement and glass matrix, respectively, for synthesis of this novel GRFG composite. Fine soda lime powders have a low glass transition temperature (T_g) of 564–573 °C with 4 μm in size [15]. Borosilicate S-glass fibers with T_g of 815 °C [16] with $\sim$15 μm in diameter are selected as fiber reinforcement due to their high strength at high temperatures and relatively low cost. During laser scanning, most of the laser energy is absorbed by fine glass powders due to multiple laser ray reflections, whereas the glass fibers are largely transparent to the 1070 nm wavelength fiber laser. Due to the laser heat absorption, fine glass powders turn into viscous flow. The molten glass flows through and encapsulates the relatively solid fibers, which are not fused due to their relatively higher glass transition temperature. To preserve the fiber morphology and mechanical strength during the SLM process, temperature of the viscous molten glass flow must be well controlled within the range of 573 °C to 815 °C. Upon cooling, a compacted GRFG composite forms with a high volume ratio of intact and well-encapsulated glass fibers. Post-process analyses are performed to investigate the microstructure of the GFRG composite and fusion bonding mechanism at the glass fiber-glass matrix interface.

2. Experiments

An experimental setup was developed for SLM of GFRG composites using a multi-mode 500 W continuous waveform Ytterbium fiber laser (IPG YLR-500-MM-AC-Y11, 1070 nm). As illustrated in Fig. 1a, laser raster scan of a wide range of speed, i.e., 1 mm–1000 mm/s, was implemented using a laser scan head

* Corresponding author.
E-mail address: hongtao-ding@uiowa.edu (H. Ding).

https://doi.org/10.1016/j.mfglet.2017.09.001
2213-8463/

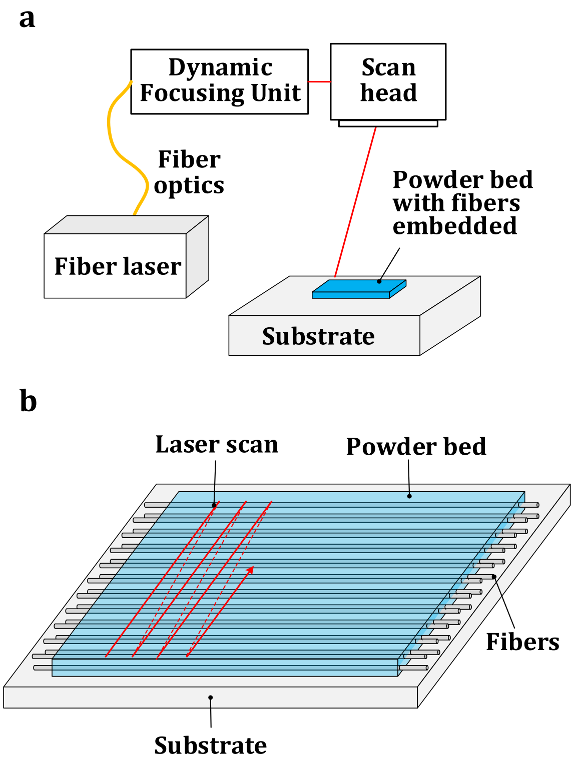

Fig. 1. Design of SLM experiments: (a) SLM setup; (b) unidirectional fiber layout.

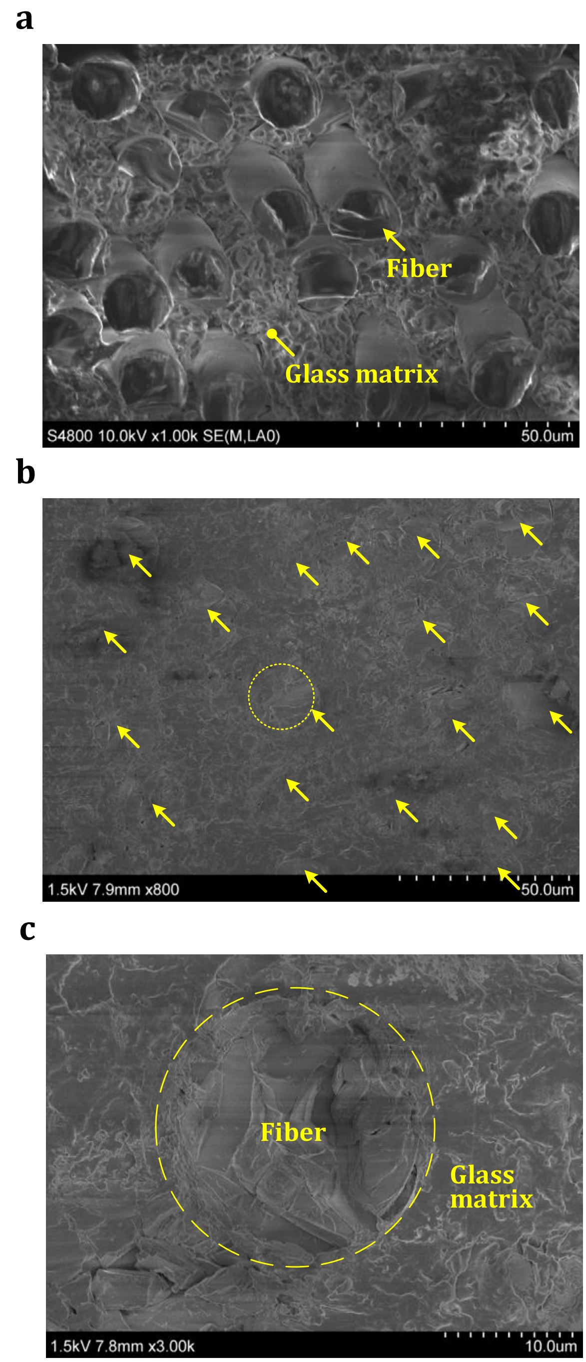

Fig. 2. Transverse sections of unidirectional GFRG composite samples. (a) Single scan, $P = 135$ W, $v = 2.5$ mm/s; (b) raster scan, $P = 80$ W, $v = 1.25$ mm/s; (c) raster scan, microstructure around a fiber.

(SCANLAB intelliSCAN 20) in conjunction with a dynamic focusing unit. During the SLM experiments, one layer of GFRG composite was fabricated to evaluate the feasibility of this process (Fig. 1b). Fine glass powders were manually applied with the fiber bundles before laser scan. A transparent borosilicate glass slide was placed on top of the powder bed to avoid any balling effect during SLM. Due to various amount of fibers placed for each layout, the thickness of powder layer was about 0.3–0.5 mm. For these experiments, the laser power (P) ranged from 50 W to 250 W, and the scanning speed (v) ranged from 1 mm/s to 60 mm/s. The laser spot size was set to 5 mm, and a raster scan width was set to be 2.5 mm, i.e., a 50% overlap.

After the experiments, the fabricated GFRG composite specimens were mounted in acrylic resin, and sectioned using a diamond saw. Scanning electron microscopy (SEM) analysis was performed to investigate the fusion microstructure and fracture mechanism. The sectioned samples were intentionally not polished flat to preserve the fibers and fractured surface.

3. Results and discussions

Fusion bonding between glass fiber and glass matrix was investigated using the unidirectional GFRG composite specimens fabricated using various laser processing conditions. Using a single laser scan with power of 135 W and speed of 2.5 mm/s, a unidirectional GFRG composite specimen was successfully fabricated. As shown in Fig. 2a, it can be observed that glass powders were completely fused to form the solid glass matrix. S-glass fibers were remained intact and well-encapsulated by the glass matrix. Few defects can be observed in the glass matrix and at the fiber-matrix interface.

A raster laser scan condition produced a significantly different fusion microstructure as shown in Fig. 2b and c. Under this condition, an even sectional specimen surface was obtained after saw cutting. Examined under a low magnification of 800x (Fig. 2b), the SEM micrograph shows about 20 fibers (indicated with arrows) randomly distributed within an area of about 110 × 150 μm^2 without fiber pull-outs or porosity. The fiber volume ratio was estimated to be at least 38% under this condition. The fiber–matrix interface can only be resolved under a high magnification of ~3000× (Fig. 2c). A brittle fractured fiber can be clearly identified (indicated by the circle), whereas the surrounding fused glass matrix shows a ductile fracture. The indistinguishable fiber-glass matrix interface indicates the fiber surface was completely well fused with glass matrix. A defect-free bonding interface can be inferred under this condition. These findings demonstrated that the fibers are remained intact during the SLM process by a proper

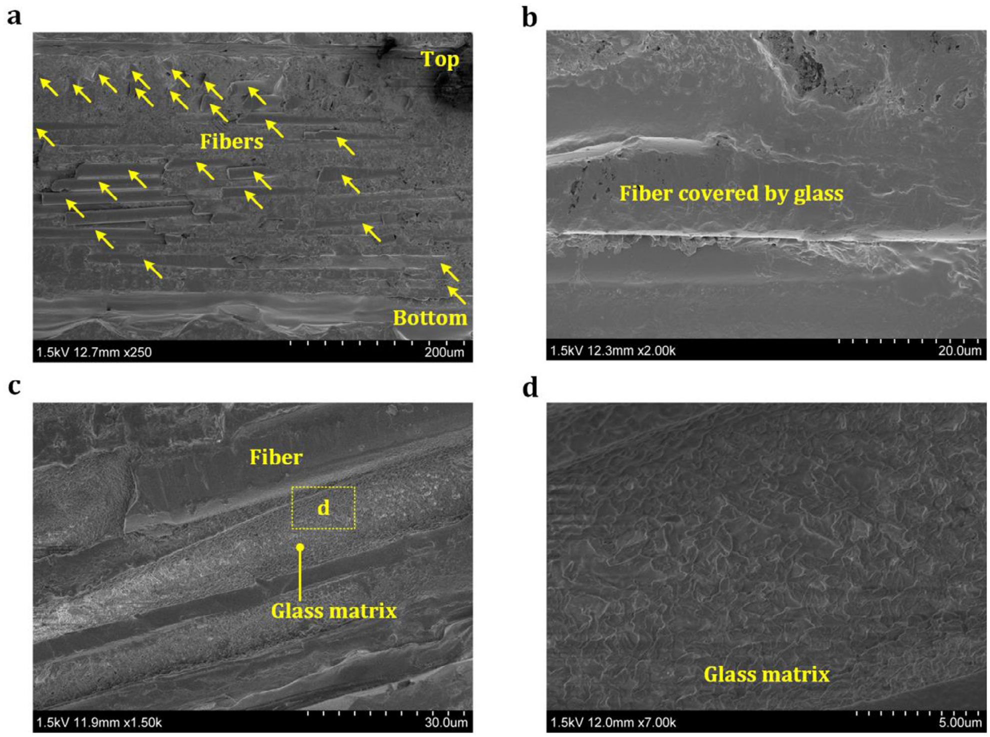

Fig. 3. Unidirectional GFRG composites formed with raster scan ($P = 80$ W, $v = 1.25$ mm/s). (a) Longitudinal section of the specimen; (b) detailed view of a fiber encapsulated by glass matrix; (c) glass matrix after fiber removal; (d) detailed microstructure of the glass matrix after fiber removal.

control of the laser process parameters, while the glass powders can be completely fused to form a solid defect-free glass matrix.

The fusion microstructure and fracture mechanism were further investigated for the unidirectional GFRG composite samples formed by raster scans. In the longitudinal section as shown in Fig. 3a, many fibers can be seen encapsulated by the fused glass matrix without significant pores. Due to the sample preparation process using saw cutting, fibers on the sectional surface were broken with a brittle fracture characteristic, while glass matrix shows a ductile fracture characteristic. As shown in Fig. 3b, some fibers remain encapsulated within the glass matrix. The fracture occurred in the glass matrix, not at the fiber-matrix interface, and left a large amount of residual glass matrix material on the fiber surface. Some fibers were completely removed from the glass matrix as shown in Fig. 3c, and cylindrical glass matrix fractured surfaces were exposed. Examined under a high magnification, the SEM micrograph of the fractured glass matrix shows a homogeneous texture (Fig. 3d). This microstructure analysis showed that a ductile fracture occurs in the glass matrix around a fiber, rather than at the fiber-matrix interface. Compared with the fusion microstructure achieved from single scan, a higher quality bonding was formed under the raster scan condition and was likely to be caused by a higher molten glass temperature.

The material transport process for this SLM process is governed by viscous flow, capillarity, and solidification. The molten glass is very viscous in nature [17–19], and its flow significantly depends on the volume fraction of fibers and their arrangement [20–22]. The current study demonstrates the feasibility of a high-viscosity molten glass flow through the random fibrous media during this new SLM process for manufacturing of GFRG composite material. A fundamental understanding of the process mechanism will be further investigated in future study. It is worth noting that this method has a great potential to be transformed to other FRP composites or metal matrix composites.

4. Conclusions

Manufacturing of FRG composite was demonstrated using a new SLM process. High-fiber volume ratio GFRG composites were successfully synthesized using borosilicate S-glass fibers and fine soda lime glass powders. The microstructural analysis showed the fibers are remained intact during the SLM process by a proper control of the laser process parameters, while the glass powders can be completely fused to form a solid defect-free glass matrix. A good bonding was formed at the fiber-matrix interface. Fracture analysis showed that a ductile fracture occurs in the glass matrix, rather than at the fiber-matrix interface.

Acknowledgements

The authors gratefully acknowledge the financial support by the National Science Foundation under Grant Number CMMI-1537512.

References

[1] Brennan JJ, Prewo KM. Silicon carbide fibre reinforced glass-ceramic matrix composites exhibiting high strength and toughness. J Mater Sci 1982;17(8):2371–83.
[2] Iba H, Chang T, Kagawa Y, Minakuchi H, Kanamaru K. Fabrication of optically transparent short fiber reinforced glass matrix composites. J Am Ceram Soc 1996;79:881–4.
[3] Dericioglu AF, Kagawa Y. Improvement of fracture resistance in a glass matrix optomechanical composite by minicomposite unit bridging. Mater Sci Eng, A 2005;406(1–2):142–51.
[4] Hülsenberg D, Fehling P, Leutbecher T. Damage tolerant, translucent oxide fiber/glass matrix composites. Compos B Eng 2008;39(2):362–73.
[5] Boccaccini AR, Atiq S, Helsch G. Optomechanical glass matrix composites. Compos Sci Technol 2003;63(6):779–83.
[6] Desimone D, Dlouhy I, Lee WE, Koch D, Horvath J, Boccaccini AR. Optically-transparent oxide fibre-reinforced glass matrix composites. J Non-Cryst Solids 2010;356(44–49):2591–7.
[7] Bernardo E, Stoll E, Boccaccini AR. Novel basalt fibre reinforced glass matrix composites. J Mater Sci 2006;41(4):1207–11.

[8] Raab D, Pfeifer K, Hülsenberg D, Boccaccini AR. Mechanical properties of oxide-fiber reinforced glass matrix composites with BN or SnO_2 interfaces. Mater Sci Eng, A 2006;417(1–2):341–7.
[9] Tan H, Satoh G, Yao YL. Through thickness laser joining of continuous glass fiber fabric reinforcement. 31st Int. Congress on Applications of Lasers and Electro-Optics (ICALEO '12), Aneheim, CA.
[10] Tan H, Yao YL. Feasibility analysis of inter-laminar toughening for improving delamination resistance. Manuf Lett 2013;1(1):33–7.
[11] Tan H, Lawrence Yao Y. Laser joining of continuous glass fiber composite preforms. ASME J Manuf Sci Eng 2013;135(1):11010.
[12] Bian D, Satoh G, Lawrence Yao Y. The laser interlaminar reinforcement of continuous glass fiber composites. J Manuf Sci Eng 2015;137(6):61001.
[13] Klein J, Stern M, Franchin G, Kayser M, Inamura C, Dave S, Weaver JC, Houk P, Colombo P, Yang M, Oxman N. Additive manufacturing of optically transparent glass. 3D Printing Additive Manuf 2015;2(3):92–105.
[14] Luo J, Gilbert LJ, Qu C, Landers RG, Bristow DA, Kinzel EC. Additive manufacturing of transparent soda-lime glass using a filament-fed process. J Manuf Sci Eng 2017;139(6):61006.
[15] Seward TP, Vascott T. High temperature glass melt property database for process modeling. Wiley; 2005.
[16] Wallenberger FT, Bingham PA. Fiberglass and glass technology: energy-friendly compositions and applications. US: Springer; 2009.
[17] Hrma P. High-temperature viscosity of commercial glasses. Ceram Silik 2006;50(2):57–66.
[18] Stokes YM. Very viscous flows driven by gravity with particular application to slumping of molten glassno title. The University of Adelaide; 1998.
[19] Fluegel A. Glass viscosity calculation based on a global statistical modelling approach. Glass Technol – Eur J Glass Sci Technol Part A 2007;48(1):13–30.
[20] Yazdchi K, Srivastava S, Luding S. Microstructural effects on the permeability of periodic fibrous porous media. Int J Multiph Flow 2011;37(8):956–66.
[21] Gebart BR. Permeability of unidirectional reinforcements for RTM. J Compos Mater 1992;26(8):1100–33.
[22] Bruschke MV, Advani SG. Flow of generalized newtonian fluids across a periodic array of cylinders. J Rheol (1978-present) 1993;37(3):479–98.